Identification of Platinum(II) Sulfide Complexes Suitable as Intramuscular Cyanide Countermeasures

Matthew M. Behymer, Huaping Mo, Naoaki Fujii, Vallabh Suresh, Adriano Chan, Jangweon Lee, Anjali K. Nath, Kusumika Saha, Sari B. Mahon, Matthew Brenner, Calum A. MacRae, Randall Peterson, Gerry R. Boss, Gregory T. Knipp, and Vincent Jo Davisson*

Read Online

ACCESS | Metrics & More | Article Recommendations | Supporting Information

ABSTRACT: The development of rapidly acting cyanide countermeasures using intramuscular injection (IM) represents an unmet medical need to mitigate toxicant exposures in mass casualty settings. Previous work established that cisplatin and other platinum(II) or platinum(IV)-based agents effectively mitigate cyanide toxicity in zebrafish. Cyanide's *in vivo* reaction with platinum-containing materials was proposed to reduce the risk of acute toxicities. However, cyanide antidote activity depended on a formulation of platinum-chloride salts with dimethyl sulfoxide (DMSO) followed by dilution in phosphate-buffered saline (PBS). A working hypothesis to explain the DMSO requirement is that the formation of platinum−sulfoxide complexes activates the cyanide scavenging properties of platinum. Preparations of isolated $NaPtCl_5$−DMSO and $Na(NH_3)_2PtCl$−DMSO complexes in the absence of excess DMSO provided agents with enhanced reactivity toward cyanide *in vitro* and fully recapitulated *in vivo* cyanide rescue in zebrafish and mouse models. The enhancement of the cyanide scavenging effects of the DMSO ligand could be attributed to the activation of platinum(IV) and (II) with a sulfur ligand. Unfortunately, the efficacy of DMSO complexes was not robust when administered IM. Alternative Pt(II) materials containing sulfide and amine ligands in bidentate complexes show enhanced reactivity toward cyanide addition. The cyanide addition products yielded tetracyanoplatinate(II), translating to a stoichiometry of 1:4 Pt to each cyanide scavenger. These new agents demonstrate a robust and enhanced potency over the DMSO-containing complexes using IM administration in mouse and rabbit models of cyanide toxicity. Using the zebrafish model with these Pt(II) complexes, no acute cardiotoxicity was detected, and dose levels required to reach lethality exceeded 100 times the effective dose. Data are presented to support a general chemical design approach that can expand a new lead candidate series for developing next-generation cyanide countermeasures.
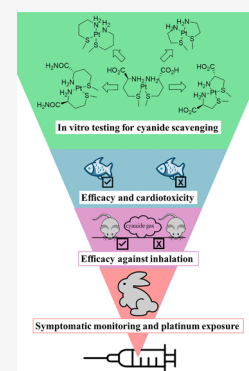
1. INTRODUCTION

Cyanide exposure may be encountered due to its widespread use in many industries and in consumer products.[1] Cyanide exposure can be fatal when small amounts are inhaled, ingested, or directly contacted.[2−4] Household fires resulting in combustion of plastics and plant-based materials, including wood, can be sources of cyanide.[2,4] As a result, cyanide is released into the smoke when carbon and nitrogen-rich materials are burned and can be readily inhaled by victims and rescue workers.[3,5,6] For example, cyanide was emitted from the burning of sound-proofing plastics associated with high morbidity and mortality events in nightclubs, claiming the lives of almost 300 victims in one single event.[7] Another critical source of cyanide exposure is industrial accidents at sites that use cyanide or cyanide derivatives in processing or manufacturing.[4,8] The relative ease of access to cyanide and cyanide precursors also elevates the risk of malicious misuse such as chemical weapons.[4,9,10]

Cyanide gas is difficult to detect and has a rapid toxic onset; within minutes, a dose of 2 mg/kg is often lethal.[5] Currently, the estimated median arrival time for ambulance services in the U.S. is 16 min.[11] Within the time required for emergency responders to arrive and administer treatment, the toxic effects of cyanide are already advanced. In the event of lethal acute cyanide exposure, mortality and morbidity occur within the first 30−60 min, thus representing an unmet medical need for rapid-acting countermeasures.[5] Common symptoms of acute cyanide exposure are headaches, unconsciousness, apnea, and death. One primary target for cyanide is the inhibition of cytochrome C oxidase activity in the mitochondria. Inhibition of this enzyme blocks cellular respiration and can manifest itself clinically as cardiac arrhythmias, seizures, behavioral disturbance, or even as an imbalance of normal oxy-/deoxygenated hemoglobin homeostasis.

FDA-approved treatments for cyanide exposure include hydroxocobalamin, sodium nitrite, and sodium thiosulfate.[12] Dicobalt edetate is used in Europe only in cases of severe cyanide intoxication due to the compound's adverse effects.[13,14] The rescue mechanism for cobalt-containing scavengers is the direct binding of cyanide to cobalt, thus reducing the inhibition of cytochrome C oxidase.[15] Hydroxocobalamin binds only one cyanide anion.[16] In contrast, cobinamide, another derivative of vitamin B12, shows promise as a cyanide scavenger that can bind two cyanide equivalents. Previous studies with cobinamide demonstrate improved efficacy in multiple animals over hydroxocobalamin when used as a cyanide countermeasure.[17−20]

Using a different pathway for cyanide detoxification, sodium thiosulfate binding mitigates conversion to thiocyanate utilizing the enzymes rhodanese or 3-mercaptopyruvate sulfurtransferase enzymes.[21] Developing cyanide scavengers with sulfur donors has shown promise including sulfanogen, tetrathionate, and dimethyl trisulfide.[21−24] Formulations of these agents offer materials that are efficacious cyanide scavengers when administered *via* intramuscular injection (IM) in large animal models.

Currently approved cyanide countermeasures are administered by IV infusion or inhalation, typically requiring trained medical staff.[16] Therefore, treatments may take substantial time for the complete administration and pharmacological action, making them less than optimal in a mass casualty event.[4,25,26] For example, 5 g of hydroxocobalamin is administered by IV infusion over 15 min, occasionally needing repeat doses.[27,28] A further complication is that compounds like hydroxocobalamin have relatively low aqueous solubility (27.3 ng/mL) that can be a confounder with multiple dosing. Moreover, due to the toxic side effects of current treatments, there is ambiguity regarding the best countermeasure options in emergencies.[27] All of the active scavenger agents currently in use are stoichiometric reactants with cyanide. This relationship increases the dosage requirement of the active pharmaceutical ingredient and imposes additional limitations on routes of administration. The discovery and development of rapid-acting cyanide countermeasures that can be delivered *via* IM administration with increased solubility and reduced side effects remain critical areas for investigation.

In the previous work, *in vivo* screens of chemical agents that rescue zebrafish from toxic levels of cyanide exposure led to the discovery of platinum-based complexes.[29] The proposed mechanism of action was based on the known interaction of platinum with cyanide to form stable complexes.[30−32] A list of 36 organoplatinum complexes including drugs such as cisplatin and oxaplatin were tested. Each sample required heating in dimethyl sulfoxide (DMSO) before dilution in phosphate-buffered saline to reveal meaningful rescue activity.[29] A key observation was that the rescue of cyanide with cisplatin occurs only with the DMSO-treated material. DMSO reactions with Pt(II)-based therapeutic agents are well known.[33−36] The cisplatin formulated with DMSO, when administered *via* the intraperitoneal (IP) route was shown to rescue mice treated with lethal doses of cyanide. Hexachloroplatinate (HCP) in this formulation was further tested in rabbit and pig models of cyanide toxicity by IP and IM administration to demonstrate the efficacy of survival from lethal cyanide exposures.[37] Evidence for forming platinum cyanates in circulation and reversal of the metabolic blockade of Krebs' cycle was observed. Intraperitoneal administration of both DMSO-treated cisplatin and HCP reversed symptoms of cyanide-induced oxyhemoglobin monitored in rabbit circulation to substantiate the reduction in toxic substance levels. These studies establish the necessary proof of concept that cyanide-reactive Pt complexes can display antidote properties in these animal models.

The prior use of platinum in pharmaceuticals in clinical settings offers some guidance in designing practical cyanide countermeasures. Cisplatin, oxaliplatin, and carboplatin are anticancer agents administered only by IV infusion. The dose-limiting toxicity of cisplatin is 20-fold higher than that of HCP, while the solubility is 33-fold lower than that of HCP.[37,38] Interestingly, DMSO with cisplatin and related drugs reduces the antitumor potency and toxic side effects.[39,40] However, the dose-limiting toxicity of cisplatin−DMSO has not been reported. Regardless, these prior observations implicate a significant role for a sulfur ligand in the efficacy of the platinum-based cyanide scavengers.

This study synthesized and evaluated three new Pt−DMSO complexes for solubility, cyanide reactivity, efficacy in rescue zebrafish, and mouse and rabbit models of lethal and nonlethal cyanide toxicity. The data define the chemical composition of the active components of the prior work using DMSO-formulated HCP and cisplatin. Furthermore, the bidentate amino-sulfide ligands' role in direct reactions of Pt(II) centers with cyanide increases the rate of addition to produce tetracyanoplatinate(II). Importantly, this reactivity directly translates to enhancements in the capacity of Pt(II) to rescue cyanide toxicity in zebrafish, mouse, and rabbit models. The variation in ligand composition opens a new avenue for further lead candidate identification for next-generation cyanide countermeasures.

2. EXPERIMENTAL SECTION

2.1. Materials and Special Equipment. $Na_2[PtCl_4] \cdot nH_2O$ ($n \sim$ 3, Premion, Pt 42.4% min) was purchased from Alfa Aesar (Tewksbury, MA). All other chemicals, solvents, thin-layer chromatography (TLC) plate (silica gel), and silica gels were purchased from MilliporeSigma (Sigma-Aldrich, Burlington, MA) or Ambeed (Arlington Hts, IL) and used as received. Smart Evaporator, an equipment capable of removing DMSO at below 50 °C under atmospheric pressure, was acquired from BioChromato Inc (Kanagawa, Japan).

2.2. Methods. *2.2.1. Generation of Platinum Complexes.* Compound **1**: *Cis*-diamminedichloroplatinate (cisplatin) was purchased from Sigma-Aldrich for use in these studies.

Compound **2**: Sodium hexachloroplatinate hexahydrate (HCP) was purchased from Sigma-Aldrich for use in these studies.

Compound **3**: A mixture of cisplatin (3120 mg, 10.4 mmol), silver sulfate (1621 mg, 5.20 mmol), deionized water (104 mL), and DMSO (3.74 mL, 52.7 mmol) was placed in a 250 mL round-bottom flask and stirred at high-speed and protected from light at ambient temperature for 5 days. The heterogeneous mixture was centrifuged in a 50 mL Falcon tube to remove silver chloride. The supernatant was collected and concentrated to 10 mL at 35 °C *in vacuo* before transferring to a 15 mL capped plastic tube and centrifugation at 7500 rpm for 2 min to remove any elemental silver precipitates. For recovery of additional **3**, the isolated precipitate was resuspended in water and clarified by centrifugation. The supernatants containing **3** were combined solutions in a 50 mL glass bottle and dried in the Smart Evaporator at 35 °C overnight. The resultant solid was triturated and washed with ethanol (3 mL repeated four times) followed by diethyl ether (3 mL repeated 3 times) and dried *in vacuo* to yield compound **3** (4.15 g) as a light gray powder. TLC: Rf 0.5 on silica gel, 1,4-dioxane/water = 4:1, UV254, and ninhydrin. Electrospray ionization-mass spectrometry (ESI-MS) (positive ion, solvent:

water and acetonitrile), calculated for $[C_2H_{12}ClN_2OPtS]^+$: 342.000673; found: 342.000084.

Compound **4**: A mixture of HCP (Na$_2$[PtCl$_6$]·6H$_2$O, 250 mg, 0.445 mmol), DMSO (252 μL, 3.55 mmol), and deionized water (252 μL) was warmed at 45−50 °C in a 20 mL glass vial for 1 h. The mixture was diluted with deionized water (4.5 mL) and evaporated using the Smart Evaporator at 30 °C for 2 h and repeated until the solvent was evaporated. The resulting yellow-orange colored residue was purified by column chromatography (silica gel, 230−400 mesh, 5 g; 2.0 cm × 3.5 cm) using a gradient of dichloromethane/acetone (4:1−1:1). A yellow-orange viscous liquid was recovered and dried by flowing argon gas over the liquid to remove the residual solvent. Then, a semisolid was obtained and finely divided before a final drying step using a vacuum to yield compound **4** (170 mg) as a yellow powder. TLC: R_f ∼0.4 on silica gel, dichloromethane/acetone =1/1, UV254, and ninhydrin. High-resolution ESI-MS (negative ion, mobile phase: acetone), calculated for $[PtCl5(DMSO)]^-$: 446.8209; found: 446.8196.

Compound **5**: Na$_2$[PtCl$_4$]·nH$_2$O ($n \sim 3$) (200 mg, 0.416 mmol) was dissolved in deionized water (910 μL) and treated with DMSO (33 μL, 0.46 mmol). The resulting homogeneous brown-colored solution was stirred overnight while protected from light at ambient temperature. The mixture became a yellow-colored solution with needlelike solid particles. The solvent was removed using the Smart Evaporator at 40 °C until dry. The yellow solid residue was extracted with 3:1 acetone/methanol (1 mL repeated three times) until the insoluble solid became almost white in color. Using this procedure allowed scale up to 6 times the initial reaction. The resultant materials were then combined and dried *in vacuo* to yield a solid material. The recovered solid was then treated with 2 mL of ethanol and dried *in vacuo* to remove residual water. Compound **5** (1.08 g) was recovered as a yellow powder. TLC: R_f 0.6 on silica gel, dichloromethane/acetone = 1:3, UV254, and ninhydrin. ESI-MS (negative ion, mobile phase: acetonitrile and water) calculated for $[C_2H_6Cl_3OPtS]^-$; 377.885281; found: 377.88677.

Compound **6**: A mixture of Na$_2$[PtCl$_4$]·nH$_2$O (2224 mg, 5.09 mmol), L-methionine (1.45 g, 9.72 mmol), and deionized water (10.2 mL) was sonicated for 5 min until all solids were dissolved. The homogeneous mixture was protected from light and proceeded at ambient temperature for 2 h and then centrifuged to remove platinum black particles generated *in situ*. The light-yellow supernatant was lyophilized overnight. The process was repeated until a light-yellow powder was obtained to yield compound **6** (3543 mg) as a light yellow powder. TLC: R_f 0.3 silica gel, 1% NaCl in water, UV254, and ninhydrin. ESI-MS (positive ion, mobile phase: water and acetonitrile) calculated for $[C_{10}H_{22}N_2O_4PtS_2]^{2+}$: 246.5334435; found: 246.53341.

Compound **7**: A mixture of Na$_2$[PtCl$_4$]·nH$_2$O (257 mg, 0.588 mmol), L-(S-methyl)cysteine (160 mg, 1.18 mmol), and deionized water (2.9 mL) was sonicated for 5 min or until all solids were dissolved. The homogeneous mixture was protected from light, stored at ambient temperature overnight, and evaporated at 35 °C using the Smart Evaporator. The resulting pale-green sticky residue was extensively triturated using sonication in ethanol (5 mL) until the mixture became a uniform suspension. A solid was isolated by centrifugation, washed with diethyl ether (2 mL repeated three times), and dried to afford compound **7** (295 mg) as a white powder. TLC: two spots, R_f 0.3 tailing and 0.6 tailing on silica gel, 1% NaCl in water, UV254, and ninhydrin. ESI-MS (positive ion, mobile phase: acetonitrile and water), calculated for $[C_8H_{18}N_2O_4PtS_2]^{2+}$: 232.5177935; found: 232.51769.

Compound **8**: A mixture of Na$_2$[PtCl$_4$]·nH$_2$O (654 mg, 1.50 mmol), L-(N-acetyl)methionine (580 mg, 3.03 mmol), and deionized water (4.50 mL) was sonicated until all solids were dissolved. The homogeneous mixture was protected from light, stored at ambient temperature overnight, and then evaporated at 40 °C to afford a light yellow pasty residue. The residue was dissolved with ethanol (2 mL) and dried *in vacuo*. The process was repeated to obtain an amorphous foam residue, divided into the following material, and dried *in vacuo* to isolate compound **8** as a pale yellow-greenish powder (985 mg).

TLC: two spots, R_f ∼0.5 and 0.7, 1,4-dioxane/water = 9/1, UV254, and ninhydrin. ESI-MS (positive ion, mobile phase: acetonitrile and water), calculated for $[C_{14}H_{26}Cl_2N_2O_6PtS_2]$: 648.47; found: 646.

Compound **9**: As a preliminary trial, a mixture of Na$_2$[PtCl$_4$]·nH$_2$O (119 mg, 0.272 mmol), L-methionine amide hydrochloride (81 mg, 0.44 mmol), and deionized water (1.36 mL) was briefly sonicated to create a homogeneous mixture. Product formation was indicated by TLC after a 30 min reaction time. A second reaction mixture of Na$_2$[PtCl$_4$]·nH2O (150 mg), L-methionine amide hydrochloride (102 mg), and deionized water (1.7 mL) was made in the same manner. Both mixtures were combined and dried using the Smart Evaporator at 35 °C overnight. The residue was triturated using a spatula and sonication in ethanol (3 mL), washed with diethyl ether (2 mL repeated two times), and dried to afford compound **9** (428 mg) as a beige-white powder. TLC: R_f 0.15 tailing on silica gel, 1% NaCl in water, UV254, and ninhydrin. ESI-MS (positive ion, mobile phase: acetonitrile and water), calculated for $[C_{10}H_{24}N_4O_2PtS_2]^{2+}$: 490.09103; found: 490.09107.

Compound **10**: Na$_2$[PtCl$_4$]·nH$_2$O (485 mg, 1.11 mmol) was dissolved in deionized water (5.55 mL) and 3-(methylthio)-propylamine (255 μL, 2.28 mmol) was added. The heterogeneous mixture was stirred at ambient temperature for 5 h. The resulting homogeneous mixture was evaporated using the Smart Evaporator at 35 °C overnight until dry. The residue was triturated using a spatula and washed with isopropyl alcohol (3 mL repeated three times) using a sonicator, followed by diethyl ether (3 mL repeated two times), and then dried to afford compound **10** (572 mg) as a beige-white powder. TLC: R_f 0.1 tailing on silica gel, 1% NaCl in water, UV254, and ninhydrin. ESI-MS (positive ion, mobile phase: acetonitrile and water), calculated for $[C_8H_{22}N_2PtS_2]^{2+}$: 404.079402; found: 404.07977.

Compound **11**: Na$_2$[PtCl$_4$]·nH$_2$O ($n \sim 3$) (134 mg, 0.307 mmol) was dissolved in deionized water (1.5 mL) before addition of 2-(methylthio)ethylamine (57 μL, 0.61 mmol). The resulting heterogeneous mixture was stirred at ambient temperature overnight before an equal volume of 1,4-dioxane was added as a cosolvent and stirred at 35−40 °C. Any precipitate of platinum black was removed by centrifugation. The supernatant was evaporated until dried using the Smart Evaporator at 40 °C. The solid residue was washed with ethanol (1.5 mL, repeated two times) followed by diethyl ether (1.5 mL, repeated two times) and dried *in vacuo* to afford **11** (90 mg) as a light gray solid. TLC: two spots, R_f ∼0.1 tailing and 0.2 tailing, 1% NaCl in water, UV254, and ninhydrin. ESI-MS (positive ion, mobile phase: acetonitrile and water) calculated for $[C_6H_{18}N_2PtS_2]^{2+}$: 188.5279635; found: 188.52774.

2.3. Characterization and Analysis. *2.3.1. X-ray Fluorescence of Platinum.* An Epsilon 4 spectrometer (Malvern Panalytical) with a silver anode X-ray tube was used for these measurements. X-ray fluorescence spectra were collected from 1 mL of aqueous samples containing platinum complexes as analytes and manganese chloride as an internal standard. The sample mixture was pipetted onto mylar foils (ChemPlex) and embedded in 32 mm polyethylene sample cups (ChemPlex). Each sample was irradiated for 20 min. Epsilon 4 software calculated parts per million of each element from each spectrum. The ppm values for platinum were divided by the ppm value for manganese. This ratio was converted to a milligram per milliliter of platinum compared to a standard curve generated using sodium hexachloroplatinate hexahydrate. A standard K$_2$PtCl$_4$ measured at 53% within 6% of the target amount, consistent with variability observed in other compounds. The weight per volume platinum concentrations was divided by the weight per volume concentrations of complexes to g% platinum for each complex.

2.3.2. High-Performance Liquid Chromatography (HPLC). Agilent 1100 equipped with a Raptor PolarX 50 mm × 2.1 mm column was used to separate reaction mixtures of platinum. Stock solutions of each platinum complex of approximately 1 mM were prepared in 0.1 M pH 7.5 phosphate buffer. Cyanide was added to an aliquot of the platinum sample at 1, 2, 4, 7, and 10 millimolar. Three aliquots of the platinum stock were used for each concentration of cyanide. Method 1: Analysis of the starting material (**6**) used purified

water for mobile phase A and acetonitrile for mobile phase B with a gradient of 90% mobile phase B to 50% mobile phase B over 3.5 min at 0.3 mL/min. Injection volumes of 5 μL and absorption at 260 nm were used. Method 2: Analysis of cyanide reaction products used purified water for mobile phase A and acetonitrile for mobile phase B, and 10% 200 mM ammonium formate with a 0−50% mobile phase B gradient over 5 min at a flow rate of 0.3 mL/min. Injection volumes of 5 μL and absorption at 260 nm were used for all analyses. Normalized $Pt(CN)_4^{2-}$ was calculated as the difference of moles of cyanide added (x) and measured $Pt(CN)_4^{2-}$ divided by the range of $Pt(CN)_4^{2-}$ for the titration sample set.

$$\text{normalized } Pt(CN)_4^{2-} = \frac{x - Pt(CN)_4^{2-}}{Pt(CN)_4^{2-} \text{ range}} x100$$

2.3.3. Ion-Selective Electrode for the Detection of Cyanide (ISE). An Orion ion-selective electrode for cyanide was purchased from Thermo Scientific and used to quantify free cyanide in solution. The electrode was calibrated each day of use with freshly prepared cyanide standards 0.26−26.0 ppm as instructed by the product manual. Every 2 h, the electrode drift was verified to be ≤2.0%, as specified by the acceptance criteria in the manual. Titrations of the cyanide and platinum solution were performed as follows: volume of the platinum mixture containing 0.1 mM platinum and adjusted to pH >10 using NaOH to maintain cyanide in the solution. Titrations were then performed by adding small volumes equal to 1% v/v of the initial solution.

2.3.4. Ultraviolet−Visible Spectrophotometry (UV−vis). A Cary60 (Agilent) was used for all of the UV−vis experiments to monitor the reaction between platinum and cyanide. All cyanide reactions were pH 7.6 using 12.5 mM sodium phosphate with 0.8 mM KCN and approximately 0.02 mM platinum. Data collection at 24,000 nm/s between 300 and 220 nm averaging time intervals of 0.65 s for the first 30 s and once every 5 min. Kinetic data were fit using a one-phase exponential curve to derive apparent rate constants.

2.3.5. Characterization of Pt Complexes by NMR. ^{195}Pt spectra were acquired using a Bruker DRX 500 MHz spectrometer equipped with a BBFO probe operating at room temperature. ^{1}H and ^{13}C spectra were acquired using the same spectrometer or a Bruker Avance 800 MHz spectrometer equipped with a cryo-TCI probe at 25 °C. The water-soluble Pt(II) complexes were prepared at 20 to 100 mM in an aqueous buffer containing 10% D_2O. The low water solubility complex MetPt(II)Cl$_2$ was prepared at 50 mM in d_7-DMF. ^{195}Pt spectra have a spectral width of 933 ppm with a center at −3600 ppm (or −2800 ppm for MetPt(II)Cl$_2$ in d_7-DMF). Excitation angles were about 50−60° with an acquisition time of 0.16 s and a recycling delay of 0.7 s, and the total number of scans was 2048. Exponential window functions with 50 Hz line-broadening were applied to FIDs prior to Fourier transformation, manual phasing, and automatic baseline corrections.

2.3.6. ICP-MS Digestion. In 15 mL polypropylene centrifuge tubes, 90 μL of rabbit blood samples were mixed with 800 μL of 30% v/v hydrogen peroxide (Marcon Fine chemicals). Subsequently, 800 μL of Aristar ultrapure hydrochloric acid and 400 μL of Aristar ultrapure nitric acid were added. The addition of reagents to blood samples resulted in vigorous bubbling. The solutions were loosely capped and incubated at room temperature until bubbling ceased. The solutions were then heated in a water bath at 60 °C for 16 h. Each sample was diluted with MilliQ water to 10 mL, gently centrifuged at 1000g for 5 min to sediment particulates, and then transferred to new 15 mL polypropylene tubes. These samples were analyzed by inductively coupled plasma-MS (ICP-MS).

2.3.7. Quantification of Platinum by ICP-MS for Pharmacokinetics. A mass spectrometer was used in all ICP-MS analyses. Mass offsets were calculated using a multielement standard containing Au, Ir, Os, Pd, Pt, Re, Rh, and Ru in 10% hydrochloric acid (VWR). Samples were introduced into the mass spectrometer using an Arridus peristaltic pump. Samples were analyzed with take-up times of 90 s and sample collection times of 90 s each. Platinum-195 peak intensities were averaged over the sample collection time. These

averaged values were converted to nanograms per milliliter using standard curves generated with sodium hexachloroplatinate hexahydrate diluted in rabbit serum.

2.4. Efficacy Testing. *2.4.1. Zebrafish Cyanide Assay.* Zebrafish larvae were plated into 96-well plates 6 days post fertilization in HEPES-buffered Tubingen E3 medium ($n = 5$ per well). The larva was dosed in each well with potassium cyanide (50 μM) and each platinum complex (1−250 μM). The cyanide concentration represents LD100 for all embryos in each well, and survival was documented after 4 h of exposure post-treatment.

2.4.2. Cyanide Inhalation Model for Mice. Mice were placed in a gastight chamber and exposed to a lethal concentration of cyanide gas. After 15 min, the mouse was removed, injected with an antidote, and placed back into the cyanide chamber for an additional 25 min. This represents a real-life scenario of people being exposed to cyanide gas in a difficult-to-access enclosed space such as a factory or subway station, with 15 min required for emergency medical personnel to arrive at a disaster scene and 25 min to treat and evacuate the victims simultaneously.

2.4.3. Nonlethal Rabbit Cyanide Exposure. The rabbits were ventilated with 100% O_2 supply throughout the experiment. The sublethal amount of cyanide was infused for 55 min (0.167 mg/min), and the antidotes were injected intramuscularly after cyanide infusion. *In vivo* tissue oxygenation status changes were monitored non-invasively with continuous wave near-infrared spectroscopy (CWNIRS) for the following 90 min post antidote injection.

2.4.4. Zebrafish Cardiotoxicity Assay. TubigenAB zebrafish embryos (bred in-house) were incubated with each compound at the indicated doses (Table 2). A control group received water as a vehicle for 2 hours to assess heart rate changes. The heart rate changes observed for each compound were normalized to the control group for comparison. Additionally, dofetilide is used as a positive control that demonstrates the atrioventricular 2:1 block. The heart rate was measured in 15 s intervals by video. Atrial and ventricular heart rates were calculated from the average pixel density in the region of interest over time. Fast-Fourier Transform was performed to determine the heart rate, and the AV concordance was estimated.

2.4.5. Muscle Toxicity Testing. A comparative muscle toxicity study was performed to compare platinum complexes **4** and **6** to contrast with previous results observed with hexachloroplatinate in DMSO. CD-1 mice were acquired from Envigo (Indianapolis, IN) at age 3−4 weeks, with a weight range of 18−20 g for this study. In two separate studies, each complex was administered at 17 mg Pt/kg and 11.3 mg Pt/kg to males ($n = 2$ for each dose) and females ($n = 2$ for each dose) *via* IM injection into the gastrocnemius muscle. The injection samples were 50 μL solution of **4** or **6** containing Ca^{2+} and Mg^{2+}-free PBS. Studies were performed at the Purdue Translational Pharmacology and Clinical Veterinary Pathology Laboratories with full IACUC approval. Animals were humanely euthanized following the PHS Policy on the Humane Care and Use of Animals 1 and 5 days after dosing. After euthanasia, the gastrocnemius muscle was surgically removed and fixed for necropsy and histopathological analysis by Dr. Mario Sola in the Purdue Histopathology Core Facility. A written report of the observations was provided describing any changes in the tissue specimens comparative to a control.

3. RESULTS

3.1. Platinum Complexes. Previously, cisplatin and sodium hexachloroplatinate (HCP, Na$_2$[PtCl$_6$]) were found to be active as cyanide antidotes only when formulated with dimethylsulfoxide (DMSO).[29] Based on the known reactivity of platinum and DMSO, a logical hypothesis was that DMSO served as a ligand on platinum and facilitated rapid substitution for cyanide in the metal.[41,42] The DMSO complex of cisplatin (**3**) is known to have reduced toxicity and efficacy as a DNA damaging agent.[39,40] A method to prepare the sulfate salt of cisplatin−DMSO **3** from **1** made use of silver sulfate to capture released chloride to promote full conversion (Figure 1). Two
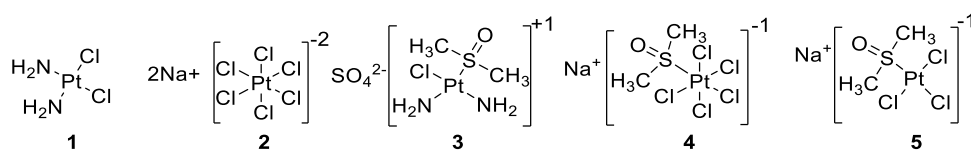
Figure 1. Starting materials and DMSO complexes under investigation as cyanide antidotes.

additional DMSO complexes **4** and **5** were also prepared from **2** and sodium tetrachloroplatinate, respectively, for further chemical and pharmacological evaluation. The preparation of complex **4** using Pt(IV) was in analogy to the original formulation used to prepare the cyanide antidotes. Compound **4** could be isolated from simple column chromatography after exposure to excess DMSO. In addition, a similar protocol was used to prepare **5** from the reaction of DMSO with tetracholoplatinate. Materials **3**−**5** had solubilities of >50 mg/mL in water, making them all suitable for pharmacological evaluations.

In the previous screening efforts, the platinum(II) complex with the two dimethylsulfide ligands was able to provide rescue from cyanide toxicity in the zebrafish model in the absence of DMSO. PBS and DMSO solvated compounds were equally efficacious showing a 2-fold greater potency with respect to cisplatin prepared in DMSO.[29] Based on the established chemical hypothesis that sulfur ligands can direct the reactivity of nucleophilic substitution at Pt(II), additional complexes were prepared to serve as improved cyanide scavenging agents.

A preliminary study was designed to guide the criteria for ligand selection of sulfur-containing Pt(II) complexes. Naturally occurring sulfhydryl, sulfide, and sulfoxide ligands/ metabolites were tested as replacements for DMSO in combinations with **2** using the zebrafish cyanide toxicity model (Table S1). A mixture of **2** with either L-methionine or S-methyl-L-cysteine in water at a 1:1 or 1:10 (Pt to ligand) ratio provided cyanide rescue in zebrafish. The potencies observed were >4-fold improved than those observed in the original DMSO formulations. In the case of compounds with free sulfhydryl (L-cysteine and L-glutathione reduced), the 1:1 mixture enhanced rescue potencies. Still, this activity was lost when the ligands were in molar excess. Finally, **2** in mixtures with sulfoxide amino acids (L-methionine sulfoxide or L-alliin) did not provide any cyanide rescue activity. Although promising, the potential of **2** to oxidize naturally occurring sulfur-containing amino acids while complexed is a known process.[43] As a result, sulfide ligands for Pt(II) complexes offered an alternative focus for designing additional candidate cyanide antidotes.

The water solubilities of Pt(II) complexes were used as a second criterion for selecting candidates. Neutral complexes showed substantially reduced solubilities in aqueous conditions, thus limiting utility. For instance, a 1:1 mol ratio mixture of L-methionine and $Na_2[PtCl_4]$ in water generated an insoluble precipitate, which was identified as a monoadduct (H-Met-OH)PtCl$_2$, a known neutral Pt(II) complex.[44] In contrast, the mixture with 2 mole equivalents of L-methionine in water was homogeneous, indicating that the monoadduct rapidly reacts with methionine to generate a bis-adduct **6** (Scheme 1). Analogously, the bis-S-methyl-L-cysteine (**7**) ligand complex was prepared. A series of Pt complexes with modifications of the carboxylate and amino groups, including N-acetyl-L-methionine (**8**), L-methionine amide (**9**), 3-(methylthio)propylamine (**10**), and 2-(methylthio)ethylamine

Scheme 1. Structural Representation of Pt Amine−Sulfide Containing Complexes Isolated and Pharmacologically Evaluated in this Study[a]
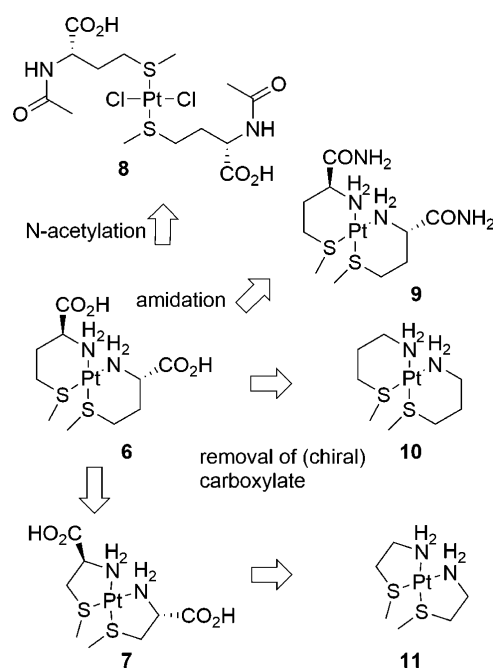
[a]Structures represent a major isomer assigned based upon heteronuclear NMR spectra consistent with prior studies on related materials.

(**11**) were prepared for comparing the structural variation impact on reactions with cyanide.

Sulfide ligands to platinum are expected to yield strong interactions.[44−48] Each of the sulfide complexes **6−11** were prepared in water before isolation as dried powders. No attempts were made to remove the sodium salt by-products. There are several isomeric species anticipated based on the ligand structures. Except for complex **8**, all of the ligands have nitrogen centers capable of bidentate coordination with Pt in square planar configurations. Previously detailed assignments guided the assignments of the major isomeric form of Pt complexes.[44] Using NMR characterization of aqueous solutions, the assignments of the major structures were made as represented in Scheme 1. For freshly prepared samples of **6** with pH 5.7, ^{1}H NMR indicates that the complex is almost exclusively *cis*, without detectable *trans*. A 9:1 mixture of *cis* to *trans* forms was identified after 6 days of storage at room temperature (RT) by ^{1}H NMR. [195]Pt NMR resonances of the *cis* form are reported to be centered upfield of the *trans* but were difficult to clearly define at 11.7 T.[44,49] The pH dependence of **6** [195]Pt NMR indicates that open ring forms dominate at low pH. In contrast, the closed forms were dominant at pH >5.7.[44] The [195]Pt NMR spectra for complex **8** in aqueous solutions indicate a significant degree of heterogeneity with at least four distinct species. Material **8**

Table 1. Evaluation of Countermeasures by Monitoring Reactions to Cyanide *In Vitro*[a]

ID	empirical formula	free cyanide removed by platinum $\frac{\text{total CN}^- - \text{free CN}}{\text{moles Pt}}$	rate of $Pt(CN)_4^{2-}$ formation k_{obs} (min⁻¹)	HPLC analysis: percent $Pt(CN)_4^{2-}$ produced	
				4 mM cyanide % (mean ± SD)	1 mM cyanide % (mean ± SD)
1	$(H_3N)_2PtCl_2$	0.4 ± 0.3	$<1.0 \times 10^{-2}$		
2	$Na_2[PtCl_6]\cdot6H_2O$	0.0 ± 0.0	$<1.0 \times 10^{-2b}$		
3	$[(H_3N)_2PtCl(DMSO)]^+ + \frac{1}{2} SO_4^{2-}$	1.5 ± 0.1	0.02 ± 0.01	61 ± 0.5	4 ± 0.4
4	$Na^+[PtCl_5(DMSO)]^-$	1.1 ± 0.2	$1.4 \times 10^{-2} \pm 1.6 \times 10^{-3b}$		
5	$Na^+[PtCl_3(DMSO)]^-$	2.1 ± 0.4	$2.4 \times 10^{-1} \pm 2.0 \times 10^{-2}$	22 ± 0.5	7 ± 0.2
6	$[(H\text{-Met-OH})_2Pt]^{2+}$ 2Cl⁻·2NaCl	4.0 ± 0.3	>15	99 ± 1.4	25 ± 0.4
7	$[(H\text{-}(S\text{-Me}) \text{ Cys})\text{-OH}_2Pt]^{2+}$ 2Cl⁻· 2NaCl	3.7 ± 0.7	$6.24 \pm 2.9 \times 10^{-1}$	84 ± 1.1	18 ± 0.7
8	$[(Ac\text{-Met-OH})_2PtCl_2]\cdot2NaCl$	1.6± 1.2	$2.1 \times 10^{-1} \pm 2.6 \times 10^{-2}$	84 ± 0.9	6 ± 0.4
9	$[(H\text{-Met-NH}_2)_2Pt]^{2+}$ 2Cl⁻·2NaCl	0.8 ± 0.2	>15	89 ± 0.7	19 ± 0.1
10	$[(CH_3SCH_2CH_2CH_2NH_2)_2Pt]^{2+}$ 2Cl⁻· 2NaCl	3.2 ± 0.6	>15	69 ± 0.03	16 ± 0.002
11	$[(CH_3SCH_2CH_2NH_2)_2Pt]^{2+}$ 2Cl⁻· 2NaCl	3.9 ± 0.2	>15	55 ± 0.09	15 ± 0.004

[a]Observed rate constants acquired under pseudo-first-order conditions with 10 molar equivalents of cyanide, product formation monitored at 255 nm for $Pt(CN)_4^{2-}$. Cyanide was quantified using an ion-selective electrode measuring the reduction of free cyanide after 10 min; platinum content was adjusted using the XRF values to correct concentrations. HPLC data were collected within 24 h of preparation, equilibrium was presumed to be established at the time of collection. [b]Rate data for Pt(IV) complexes **2** and **4** were established from the disappearance of the signal at 275 nm.
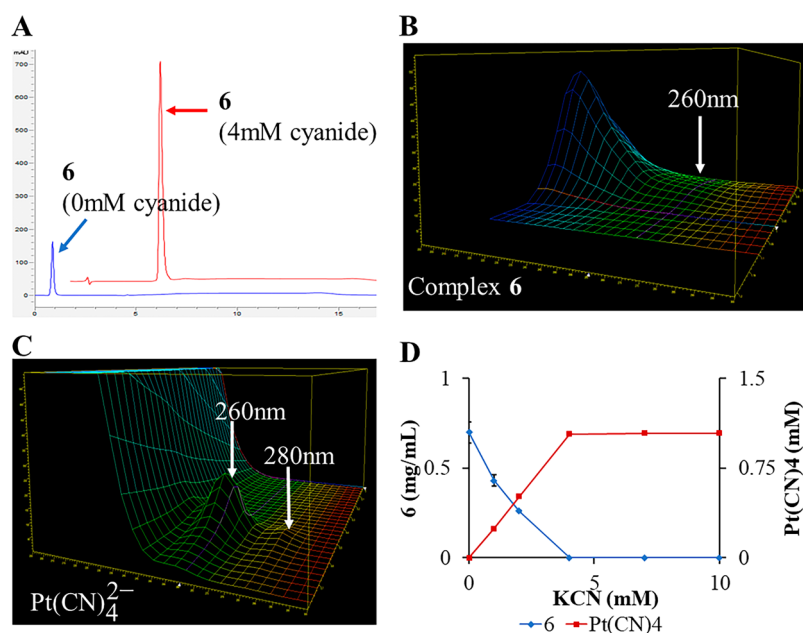

Figure 2. Reaction between platinum and cyanide monitored by HPLC. (A) Complex **6** (blue trace) and the product with cyanide (red trace) were quantified using a Restek Ultra IBD. (B, C) Photodiode array (200−300nm) of **6** shown as the blue trace in panel A. (C) Photodiode array (200−300 nm) of $Pt(CN)_4^{2-}$ having a strong charge transfer band at 260 nm consistent with the formation of $Pt(CN)_4^{2-}$. (D) Complex **6** was titrated with 1−10 molar equivalents of cyanide.

undergoes sulfide ligation but is anticipated to be an open form due to the acetylation of the amine site. Furthermore, the mass spectral analysis of the material was not indicative of a single component. This distinction serves as a basis for comparing the role of bidentate ligands.

3.2. Platinum Content and Reactions with Cyanide. Quantification of the platinum content (%w/w) in each of the sulfur-containing complexes was obtained by X-ray fluorescence (XRF). Example XRF spectra are shown in Figure S1, and the Pt(IV) and Pt(II) core excitations are distinct from the internal manganese standard. The XRF results reveal that the bulk materials for complexes **6−11** were 20−30% w/w Pt, as

summarized in Table S4. Regardless of any anticipated speciation, these values were used as the basis for the available platinum mass in each animal dose.

Each of the sulfur-containing Pt complex capacities to act as cyanide scavengers were evaluated using *in vitro* reactions with KCN. Direct scavenging of cyanide in solutions was monitored using three different methods. An ion-selective (cyanide) electrode (ISE) assay was used to evaluate the consumption of free cyanide in the presence of Pt(II) complexes.[50] After adding the platinum-containing materials at 50 μM in 0.5 mM cyanide pH >10 with 0.1 M ionic strength, the time before reading was limited to 10 min to better mimic conditions for

rapid scavenging. A summary of the amount of cyanide reduction per mole of the platinum present is in Table 1. Time-dependent UV−vis observations of the same Pt samples in the Pt/cyanide ratio of 1:40 provide estimates for the relative rates of the starting material disappearance for **2** and **4**. The dominant product of these Pt(II) complexes in a reaction with excess cyanide is expected to be $Pt(CN)_4^{2-}$. Formation of a highly stable $Pt(CN)_4^{2-}$ is based on strong field ligand properties from cyanide, exhibiting strong d-orbital splitting of the platinum core.[31,51,52] For all of the cases, **1**−**11**, the sulfur, amino, and chloride ligands are anticipated to be displaced by free cyanide. In Table 1, **6**, **7**, **10**, and **11** all appear to approach the expected consumption of 4 mole equivalents of cyanide. Product formation was also observed at 255 nm in the UV−vis assay for **3**−**11** consistent with the formation of $Pt(CN)_4^{2-}$. ISE assay conditions were highly alkaline and at a high ionic strength to maintain cyanide in solutions. At longer incubation periods (>10 min), **4** showed a larger fraction of cyanide consumption (Table S5), indicating incomplete scavenging in the ISE assay after 10 min. Complexes **8** and **9** were less reactive under the same alkaline conditions. The sulfur effect on the reactions with cyanide is highlighted by the reduced scavenging for **1** and **2** (Table 1). The ISE assay for 10 min also reveals that sulfide complexes (**6**, **7**, **10**, and **11**) were superior to the DMSO complexes (**3**−**5**) for scavenging cyanide. Similarly, time-dependent changes in UV−vis show that the most active complexes in the ISE assays also had faster apparent rates of reaction. Complexes **6**, **7**, **9**, **10**, and **11** had 10−100-fold faster observed pseudo-first-order reaction rates over the DMSO complexes under conditions some of which exceed the rate limit of manual mixing and data collection.

An HPLC method was developed to monitor the direct production of $Pt(CN)_4^{2-}$ from reactions of complexes **3**, **5**−**11**, and cyanide (Figure S2). The example data for the reaction of **6** with cyanide are shown in Figure 2A with the blue trace showing the starting material and the red trace after adding four equivalents of KCN. Complex **6** and $Pt(CN)_4^{2-}$ have discrete retention times, and the spectrum for complex **6** (Figure 2B) has no appreciable absorbance at 260 nm, where the product of the cyanide reaction shows a charge transfer band (Figure 2C). The HPLC data demonstrate that depletion of complex **6** correlates directly to $Pt(CN)_4^{2-}$ production (Figure 2D). These titrations were repeated for each of the complexes, and only the product $(Pt(CN)_4^{2-})$ was quantified. The results are normalized to maximum $Pt(CN)_4^{2-}$ observed over the titration range and are summarized in Table 1. Pt(IV) complexes were problematic due to poor compatibility with the column chemistry. Using the HPLC conditions, complexes **6**, **7**, **8**, and **9** exhibit the most significant capacity for cyanide scavenging. Close inspection of the HPLC chromatograms for **10** and **11** indicate evidence of low levels of intermediates, a possible explanation for reduced conversion to $Pt(CN)_4^{2-}$.

A third approach to analyzing the cyanide reactions with the Pt complexes **3**−**11** incorporated ^1H NMR. The results were consistent with published observations; sulfide complexes show pH-dependent spectra resulting form ring-opening and closing in the bidentate forms.[44] The ^{195}Pt NMR spectrum for **6** at pH 7.5 shows two broad peaks (Figure 3A). Adding one molar equivalent of KCN results in conversion to $Pt(CN)_4^{2-}$ (Figure 3B) in a ratio consistent with no mixed ligand intermediates. Finally, the addition of four equivalents of KCN resulted in a quantitative conversion of **6** to $Pt(CN)_4^{2-}$ (Figure 3C). These data are consistent with the direct conversion of
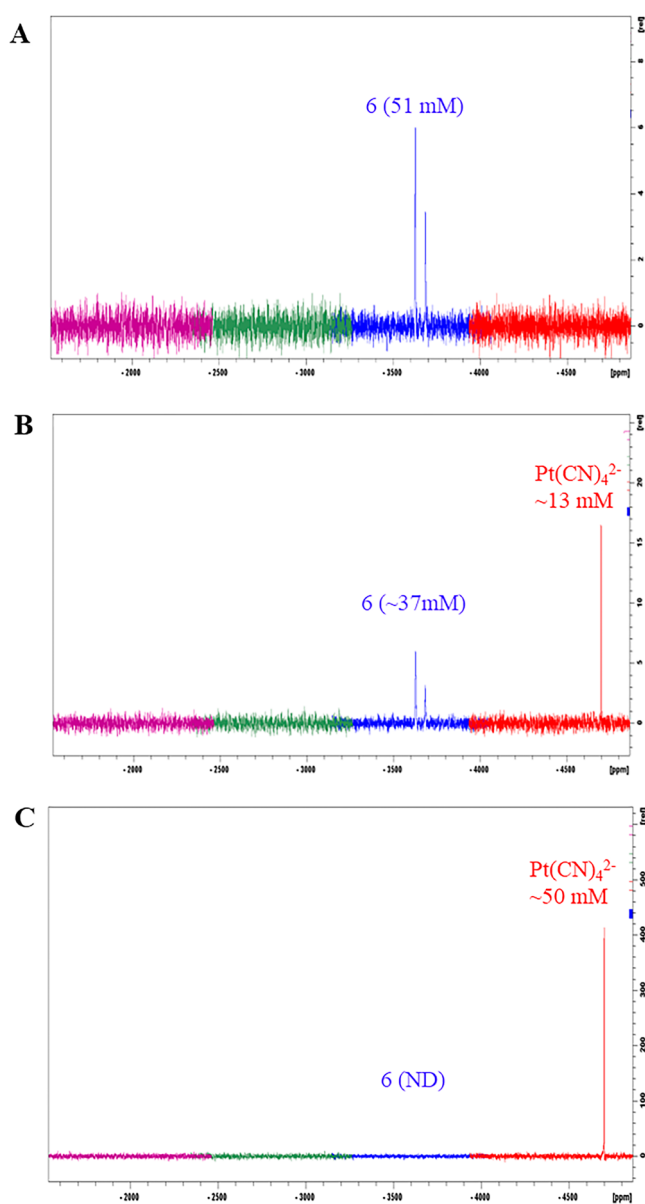

Figure 3. ^{195}Pt NMR spectra of **6** (51 mM in 200 mM sodium phosphate, 10% D_2O, pH 7.5. at 291.5 K titrated by cyanide) (A) before addition of cyanide; (B) after addition of approximately 50 mM cyanide; and (C) after addition of 200 mM (final concentration) cyanide. The observed signals correspond to the reactant ($PtMet_2$), with Pt chemical shifts around −3650 ppm, and the final product $[Pt(CN)_4^{2-}]$ with the Pt chemical shift at −4700 ppm.

the amino−sulfide Pt(II) complexes to $Pt(CN)_4^{2-}$ without the measurable existence of any mixed ligand intermediates. Each complex was also titrated with cyanide and monitored by ^1H NMR, with an example for **11** in Figure 4A−C. The release of amino sulfide or DMSO ligands can be observed by distinctive chemical shifts and reduction of line widths. All of the reaction materials in **6**−**10** showed results consistent with the direct displacement of ligands by cyanide (Figures S5−S11). Similarly, further investigation of the reduced cyanide scavenging of **9** under alkaline ISE conditions showed low conversion to the product by proton NMR (Figure S12).

The exchange of proteins with Pt(II) metallodrugs remains an area of active investigation.[53−56] Several studies have examined the interactions of amino acid side chains with
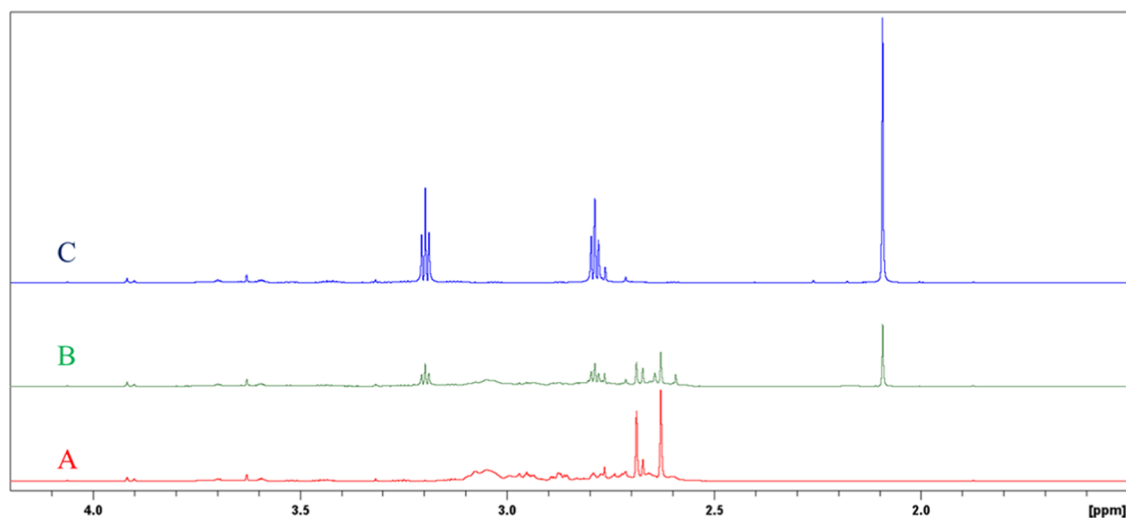
Figure 4. Pt amine−sulfide complex **11** reaction with KCN was monitored by ^{1}H NMR at 298K. (A) 1 mM compound **11** alone in 50 mM sodium phosphate, pH 7.5, 10% D_2O; (B) with 1 mM KCN added; and (C) with 5 mM (final concentration) KCN added. Ligand (2-methylthioethylamine, or MTEA) can be easily identified by the characteristic sharp peaks at 2.69 and 2.62 ppm for the bound form, and 2.1 ppm for the free form. In the absence of KCN, MTEA is found to be fully bound to Pt. Addition of KCN leads to the quantitative release of MTEA, as the signal at 2.1 ppm becomes incrementally higher in (B and C). The complete disappearance of the bound ligand is observed in (C).
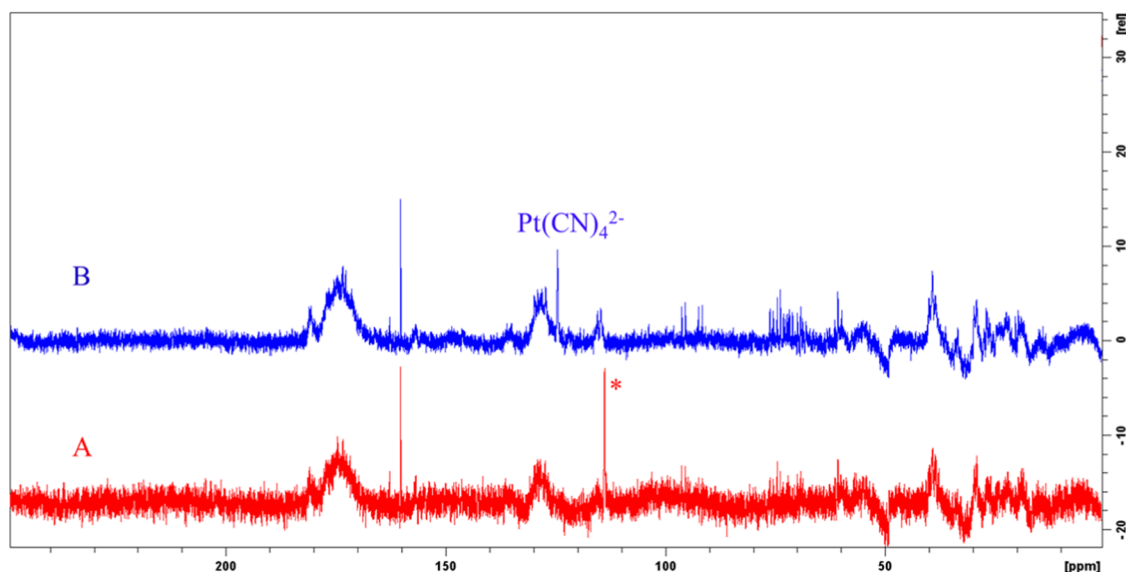

Figure 5. ^{13}C NMR of the reaction between **6** and cyanide in 100% rabbit serum. (A) Rabbit serum with 400 μM ^{13}C−KCN and (B) 100 μM complex **6** was added. The asterisk-labeled signal at 117 ppm is generated from KCN, as it exists mainly as HCN at neutral pH. The signal at 125 ppm is assigned to $Pt(^{13}CN)_4^{2-}$ while satellites from ^{195}Pt coupling are not clearly observed presumably due to the low signal-to-noise ratio and line-broadening. Semiquantitation of $Pt(^{13}CN)_4^{2-}$, based on the signal at 117 ppm (for 400 μM) suggests that its concentration is about 100 μM, consistent with the expectation of full scavenging of cyanide by compound **6**.

platinum drugs. Components of biological matrices that ligate platinum, such as thiol-containing metabolites, i.e., glutathione, might reduce platinum's capacity to scavenge cyanide. Reactions were executed in the presence of rabbit serum to assess the impact of biological matrices on the cyanide reactivity of **6** (Figure 5A−C). As a feasibility study, 100 μM of compound **6** was exposed to 400 μM [^{13}C]KCN in 100% rabbit serum, and ^{13}C NMR spectra were acquired (Figure 5). Semiquantification of ^{13}C in serum reveals that $Pt(CN)_4^{2-}$, with a signature chemical shift at 125 ppm, is the major reaction product within <1 h of mixing (if not shorter, due to the required NMR data collection time). The implication is

that the serum matrix does not significantly reduce the ability of **6** to scavenge cyanide compared to serum-free conditions.

3.3. Zebrafish Survival Model. The previous efforts to screen commercially available compounds for cyanide rescue in a lethal zebrafish model provided a path for prioritizing agents in rodent models of cyanide toxicity.[29,37] Zebrafish were used to assess the sulfur-containing Pt complexes **3**−**11** and prioritize candidate agents for further *in vivo* testing. Briefly, complexes were reconstituted in purified water and introduced to the zebrafish bath until 100% rescue was obtained (Table 2). When compiled on a per mole Pt dose formulated in DMSO, cisplatin **1** was more potent than hexachloroplatinate **2**. The same trend was observed for the isolated DMSO

Table 2. Efficacy of Countermeasures in Cyanide Challenged Zebrafish[a]

complex	$EC_{100} \frac{\mu g \, Pt}{mL}$
1	2.9^b
2	12.1^b
3	3.3
4	11.7
5	3.3
6	1.2
7	1.3
8	4.8
9	4.6
10	2.4
11	1.9
$K_2Pt(CN)_4^{2-}$	not active

[a]Zebrafish data represent EC_{100} of each complex formulation with aqueous conditions. [b]Platinum complex was predissolved in DMSO. Each result is the concentration of platinum necessary for $n = 5$ (100%) survival in the presence of 100 μM potassium cyanide, which results in death after 1 h in the control groups. The reported survival is 4 h after cyanide exposure. Toxicity in zebrafish is represented as the lethal dose in half the population (LD_{50}), which is due to the presence of the platinum complex. Toxicity is represented as the percentage heart rate of the control group; lower heart rates indicate increased cardiotoxicity ($n = 12$ per group).

complexes **3** and **4**, which were equipotent with the formulations made in DMSO. These results are consistent with the hypothesis that prior work's active Pt agent formulations contained one DMSO ligand.[29,37] In contrast to the preceding work, this analysis further demonstrates that Pt(II) complexes exhibit greater efficacy than Pt(IV) complexes. Also included for comparison is the isolated Pt(II)-DMSO complex **5**, which showed efficacy similar to **3**. In addition to the sulfur-directing effect for cyanide substitution to Pt, materials **3−5** exhibited improved aqueous solubilities that contributed to the overall cyanide rescue properties. When tested using the same zebrafish model, the amino−sulfide Pt(II) materials **6−11** reveal similar trends with complexes **6**, **7**, **10**, and **11** showing potencies comparable to cisplatin−DMSO **3**. To assess cardiotoxicity, the heart rate and atrioventricular (AV) conduction were used to screen each complex without cyanide in a validated physiological analysis Figure 6.[57,58] There was no evidence of bradycardia or the AV block observed using the EC_{100} doses of **1−11**.

3.4. Mouse Inhalation Model. While the *in vivo* zebrafish testing indicated the potential of these Pt(II) complexes to serve as cyanide scavengers, the product concept requires availability through intramuscular injection. The lethal inhalation model in mice offers a stringent test for efficacy using either IP or IM administration. The basic scheme for this established model is presented in Table 3. Mice are exposed to lethal amounts of cyanide gas and monitored for survival 25 min after injection of candidate antidotes. This model has also been used to test the efficacy of the platinum-based cyanide countermeasures.[28,35] A phosphate buffer was used to control the pH in each formulation of the different sulfur-containing Pt complexes. Despite the potency of **3** in the zebrafish model, the mouse model revealed that the material was not reproducibly effective when administered by IM injections (Table 3). This result is consistent with the previous studies with the cisplatin formulated in DMSO. When **4** was delivered
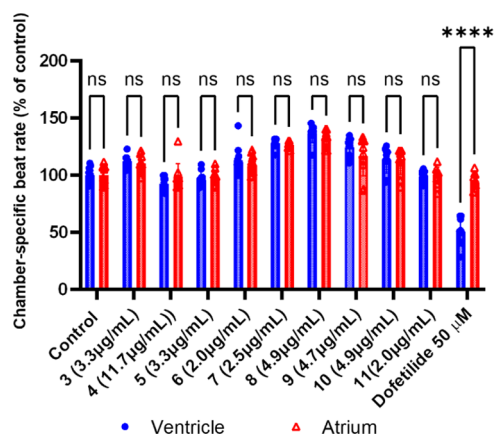

Figure 6. Cardiotoxicity testing of Pt complexes in zebrafish. This assay was performed on zebrafish embryos in the presence of Pt complex agents and dofetilide as the positive control. Target concentrations were chosen from the zebrafish cyanide rescue efficacy doses. Analysis was performed using a multiple comparison test between the means of the ventricle and atrium. The differences between the two means were not significant for all of the doses administered. $P < 0.00005$ for the dofetilide control.

Table 3. Lethal Exposure by Inhalation: Mouse[a] Mice Are Exposed to Lethal Amounts of Cyanide (LD_{100} after 40 min); after 15 min, the Mouse is Injected with the Antidote Intramuscularly and Continued Exposure for the Remaining 25 min
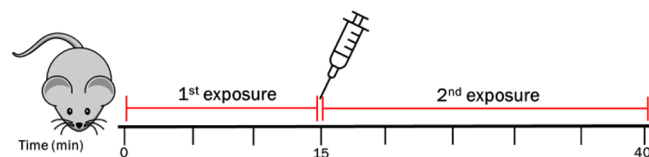
complex	dose $\frac{mg \, Pt}{kg}$	mouse survival
1	$97.5^{\text{Nath et al., IP}}$	0/6
	$195^{\text{Nath et al., IP}}$	5/6
2	17^{IP}	3/6
	$24^{\text{Nath et al., IP}}$	3/6
	$49^{\text{Nath et al., IP}}$	6/6
3	15^{IM}	2/3
	23^{IM}	0/3
	30^{IM}	0/3
	45^{IM}	1/3
4	8^{IP}	1/8
	17^{IP}	4/6
	20^{IM}	0/3
5	20^{IM}	0/3
	29^{IP}	0/3
6	9^{IM}	1/4
	11^{IM}	2/5
	17^{IM}	5/5
7	12^{IM}	1/2
	19^{IM}	5/5
8	13^{IM}	0/3
	20^{IM}	0/5
9	17^{IM}	3/5
10	20^{IM}	5/5
11	17^{IM}	5/5

IP, the efficacy was consistent with that observed for **2**.[29,37] Unfortunately, like **3**, no efficacy was observed with the DMSO complexes **4** and **5** when dosed in the cyanide-treated mice up to 20 mg Pt/kg by IM administration. Previously **2** was found to be active by IM injection in a lethal cyanide rabbit model at 10.4 mg/kg (equivalent to 41.6 mg/kg in mice). However, the potential for dose-limiting muscle toxicity was also observed at a 69 mg/kg dose in mice indicating a potentially narrow therapeutic window.

Platinum amine−sulfide-containing complexes showed a contrasting profile to the DMSO complexes when tested by IM administration. For materials **6** and **7**, the efficacy in the mouse model showed robust rescue at 17 and 19 mg Pt/kg, respectively (Table 3). Similarly, the analogues **9**−**11** showed similar potencies using IM administration. These results indicate a significant enhancement in the antidote activities for the five amine-sulfide Pt complexes relative to the DMSO-containing Pt complexes **2**, **3**, and **4**. In contrast, material **8** appeared to have no cyanide counteractivity in the mouse model using the same IM dose range. One explanation for this loss in activity is the observed heterogeneity of the Pt species in solution, decreasing bioavailability. Also, **9** appears to be a less efficient agent than the other four complexes. The results are consistent with the hypothesis that sulfur ligands on platinum enhance the efficacy of platinum as a cyanide countermeasure.[37] However, it is likely the physicochemical properties of the Pt ligands impart critical attributes to enable bioavailability in the IM dose form.

Furthermore, solutions of **6** were tested in the mouse inhalation model after standing at ambient temperature for up to 7 days. The same dose was used in the four studies with three mice on days 0, 1, 3, and 7. In all cases, survival was observed, adding more confidence that **6** would be an effective countermeasure candidate with a useful shelf-life (Table 4).

Table 4. Efficacy of 6 in Aged Samples Stability of the efficacious dose was verified by aging the formulation for 6 for 7 days with Subsequent Use in the Lethal Inhalation Mouse Model

sample age (days)	survival
0	3/3
1	3/3
3	3/3
7	3/3

3.5. Pharmacokinetics and Pharmacodynamics in the Nonlethal Rabbit Model.

Real-time monitoring of the oxygenated/deoxygenated hemoglobin by diffuse optical spectroscopy allows for a direct readout of cyanide effects *in vivo*.[59] A platform for conducting these studies in a rabbit model for cyanide toxicity enables a direct comparison of lead countermeasure candidates. A comparison of the time-dependent changes in hemoglobin states for **3** and **6** is shown in Figure 7. Upon IM delivery of **3**, the rate of change of the oxygenated/deoxygenated hemoglobin ratio in blood was re-established over the next 2 h showing a significant response in the nonlethal rabbit model (Figure 7B). For **6**, IM delivery resulted in a rapid change of the oxygenated/deoxygenated hemoglobin ratio over the next 15−20 min (Figure 7C). These data are consistent with the apparent reactivity of **6** with cyanide using *in vitro* measurements. The significant response to **3** in this nonlethal cyanide toxicity rabbit model was not
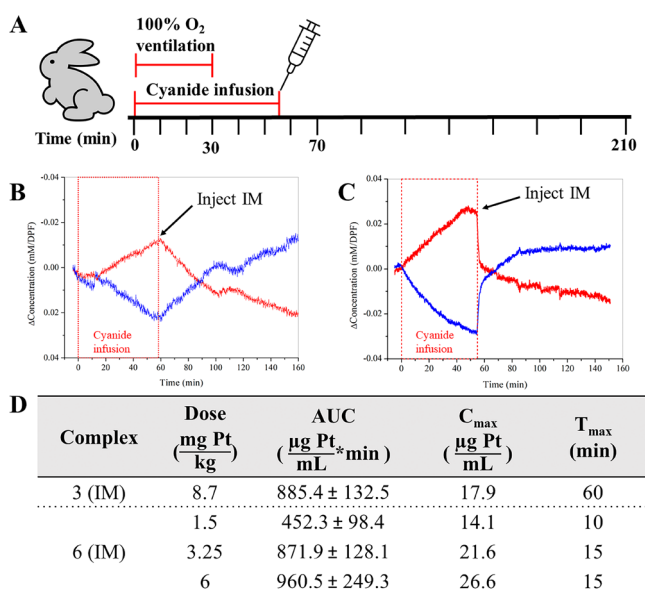

Figure 7. Complex **6** results in rapid recovery of oxy/deoxy hemoglobin. (A) Nonlethal rabbit cyanide exposure was performed with 100% oxygen ventilation for the first 30 min and infusion of sublethal cyanide over 70 min prior to injecting the drug intramuscularly. (B) Oxygenated (red) deoxygenated (blue) blood hemoglobin for rabbits treated intramuscularly with **3** after cyanide infusion shows the recovery of normal homeostatic levels. (C) Similarly, **6** was injected intramuscularly after the cyanide infusion showing a dramatic recovery of precyanide exposure levels. (D) Platinum blood plasma analysis determined by ICP-MS with AUC as the mean value of $n = 3$ replicates calculated for the first 60 min after treatment. The highest documented concentration (C_{max}) from a single injection paired with the time observed (T_{max}).

Figure 7D table:

Complex	Dose ($\frac{mg\ Pt}{kg}$)	AUC ($\frac{\mu g\ Pt}{mL}$*min)	C_{max} ($\frac{\mu g\ Pt}{mL}$)	T_{max} (min)
3 (IM)	8.7	885.4 ± 132.5	17.9	60
6 (IM)	1.5	452.3 ± 98.4	14.1	10
	3.25	871.9 ± 128.1	21.6	15
	6	960.5 ± 249.3	26.6	15

anticipated given the failure of IM administration to show meaningful efficacy in the mouse inhalation model. Analysis of the total platinum content in blood over the time course of the experiment using IM doses of **3** and **6** are compared for the AUC (Figure 7D). Dose normalization to total platinum injected shows that C_{max} levels are comparable at the higher doses. What is most distinct is the T_{max} values for 8.7 mg of **3** vs 6 mg of **6** in the total Pt dose. A direct comparison between T_{max} values suggests that the rate of absorption for complex **6** is a significant factor in achieving efficacy in both the mouse and rabbit models of cyanide toxicity.

3.6. Site of Injection Toxicity in the Mouse Model.

A prior study with $PtCl_6$ formulated in DMSO and PBS using a 69 mg Pt/kg IM dose in mice revealed significant levels of chemically induced tissue damage.[37] To assess if this toxicity will be a general limitation of the new Pt(II) complexes, complexes **4** and **6** were administered IM to six mice at 20 and 11.25 mg Pt/kg IM, respectively. These represent doses at 2.5-fold and 3-fold greater than the EC_{100} observed in the mouse cyanide inhalation model. The injection sites were monitored for significant inflammation or bruising before histopathology evaluation 5 days post-injections. In contrast to prior studies with HCP/DMSO, complex **4** at the reduced levels revealed no important pathological findings beyond the site of needle injection. Complex **6** did induce some acute myonecrosis in about 60% of the sections analyzed which appear as hypereosinophilic or swollen myofibers. The effects were localized and indicated a loss of cross striation and sarcoplasmic fragmentation on day 1 post-injection with

improvement in these sections on day 5. There were remaining signs of localized inflammatory and edematous changes at the injection site in approximately 40% of the tissue sections. The compilation of information did not indicate any significant tissue toxicity extending beyond the injection site induced by **6**.

4. DISCUSSION

As hypothesized, DMSO and related sulfur-containing ligands on platinum showed enhanced efficacy for cyanide rescue. The trans effect from sulfur in the square planar Pt(II) complexes is expected to increase the substitution rate for cyanide anions. However, there are distinctions within the shortlist of highly water-soluble formulations of sulfur-containing complexes **3**–**11**. First, the DMSO-Pt interaction in **4** exhibited poor stability in aqueous solutions as monitored by NMR (Figures S14). The reduced efficacy of **4** would be expected to contribute to the loss of platinum−DMSO interactions compromising the rate of cyanide substitution reactions.

In contrast, Pt complexes with bidentate thioether ligands (**6**, **7**, **9**−**11**) such as methionine were consistently stable in solutions and maintained reactivity toward cyanide. At higher pH, these compounds lack a positive charge on the primary amine allowing electron donation to the platinum d-orbitals contributing to resistance to hydrolysis. At lower pH values, the positively charged amine likely induces electronic repulsion to the platinum core favoring the ligation of hydroxyl or chloride. These complexes with the capacity to form ring-closed species (**6**, **7**, **9**−**11**) were also the most active cyanide scavenging agents.

As a cyanide scavenger, platinum offers potential for improved efficiency in comparison to existing metal-containing agents. Platinum complexation with cyanide is known to have a high stability constant of $\log(\beta)$ of 41 M^{-4}.[60] The data here support the rapid conversion of the bidentate ligand complexes directly to $Pt(CN)_4^{2-}$ *in vitro* when exposed to cyanide. Thus, platinum offers a greater capacity to scavenge cyanide per metal equivalent. The data are consistent with platinum's expected higher binding affinity with cyanide compared to other metal centers. For comparison, ferric iron in methemoglobin essential for cyanide detoxification has a $\log(\beta)$ of 8.7 M^{-1}.[61] Cobalt complexes have been extensively studied as cyanide scavengers as well, with stability constants of $\log(\beta)$ of 5 M^{-1} and 22 M^{-2} for hydroxocobalamin[62] and cobamamide,[63] respectively. Each of these cobalt-containing agents has a lower capacity for cyanide binding than platinum.

The bidentate amine-sulfide Pt(II) agents **6**, **7**, **10**, and **11** all showed improvements in efficacy in the zebrafish cyanide toxicity model. The mouse inhalation model showed efficacy improvements in Pt(II) doses relative to cisplatin−DMSO. The efficacious dose administered for **6** in the mouse model scales to a dose of 51 mg Pt/m^2, within the range of a single human dose of cisplatin used for oncology. Interestingly, under the time limitations of the experimental methods (NMR), there was no evidence for observable mixed cyanide−Pt(II) species. Instead, $Pt(CN)_4^{2-}$ was the only Pt(II) product under equal molar amounts of the cyanide and Pt(II) complex. The implication is that the addition of the first cyanide ligand is rate-limiting. This feature could be an essential attribute for enhancing the efficacy of Pt(II) cyanide scavenging agents. Although the isomeric species of these bidentate Pt(II) complexes that may exist in aqueous solutions could result in differences in antidote efficacy and pharmacokinetic properties,

separation and characterization of the pharmacological properties of the mixtures are beyond the scope of the current study.

Evidence from the studies presented here allows further design and optimization of the Pt(II) active cyanide countermeasures and their pharmaceutical properties. Chemical modifications of Pt(II) ligands that can balance the (i) rapid reactivity with cyanide, (ii) *in vitro* and *in vivo* stability, and (iii) solubility and bioavailability for using IM dosage forms represent a challenging set of criteria. Appropriate criteria for the selection of these new variants are in place. Using multiple animal models for cyanide toxicity with different dosing strategies highlights the utility of a tiered approach to cyanide scavenger testing. While the water bath condition for the zebrafish model cannot differentiate cyanide scavenging in the medium or the animal, the capacity to identify enhanced potency agents is further validated here. IM bioavailability in the stringent mouse inhalation model offers a clear metric for the selection of potential active candidates. Equally informative, the rabbit model offers an avenue to evaluate the candidate scavengers' relative pharmacokinetic and pharmacodynamic features, before moving to large animal models.

5. CONCLUSIONS

This study offers proof of concept for a new category of amine-sulfide Pt(II)-based cyanide countermeasures with suitable stability and IM bioavailability to warrant more advanced testing and development. In addition, potential new structural variants in the ligand design offer avenues for optimization for efficacy, safety, and developable formulations.

■ ASSOCIATED CONTENT

Data Availability Statement

All data generated or analyzed during this study are included in this published article and its Supporting Information files.

ⓢ Supporting Information

The Supporting Information is available free of charge at https://pubs.acs.org/doi/10.1021/acs.chemrestox.2c00157.

> Additional results of rescue efficacy in the zebrafish model; detailed mass and platinum content analyses; additional results of the cyanide reaction and Pt product formation assays; NMR data for the solution stability of the platinum complexes; methods calibration data; and details of specific methods (PDF)

■ AUTHOR INFORMATION

Corresponding Author

Vincent Jo Davisson − *Department of Medicinal Chemistry and Molecular Pharmacology, Purdue University, West Lafayette, Indiana 47907, United States;* ⓞ orcid.org/0000-0003-1182-0007; Email: davisson@purdue.edu

Authors

Matthew M. Behymer − *Department of Industrial and Physical Pharmacy, Purdue University, West Lafayette, Indiana 47907, United States*

Huaping Mo − *Department of Medicinal Chemistry and Molecular Pharmacology, Purdue University, West Lafayette, Indiana 47907, United States*

Naoaki Fujii − *Department of Medicinal Chemistry and Molecular Pharmacology, Purdue University, West Lafayette, Indiana 47907, United States*

Vallabh Suresh − *Department of Medicinal Chemistry and Molecular Pharmacology, Purdue University, West Lafayette, Indiana 47907, United States*

Adriano Chan − *Department of Medicine, University of California, San Diego, California 92093, United States*

Jangweon Lee − *Beckman Laser Institute and Medical Clinic, Department of Medicine, University of California, Irvine, California 92697, United States*

Anjali K. Nath − *Department of Cardiology, Beth Israel Deaconess Medical Center, Boston, Massachusetts 02115, United States*

Kusumika Saha − *Division of Cardiovascular Medicine, Brigham and Women's Hospital, Boston, Massachusetts 02115, United States*

Sari B. Mahon − *Beckman Laser Institute and Medical Clinic, Department of Medicine, University of California, Irvine, California 92697, United States*

Matthew Brenner − *Beckman Laser Institute and Medical Clinic, Department of Medicine, University of California, Irvine, California 92697, United States*

Calum A. MacRae − *Division of Cardiovascular Medicine, Brigham and Women's Hospital, Boston, Massachusetts 02115, United States*

Randall Peterson − *Department of Pharmacology and Toxicology, College of Pharmacy, University of Utah, Salt Lake City, Utah 84112, United States;* ⓞ orcid.org/0000-0003-0727-3469

Gerry R. Boss − *Department of Medicine, University of California, San Diego, California 92093, United States*

Gregory T. Knipp − *Department of Industrial and Physical Pharmacy, Purdue University, West Lafayette, Indiana 47907, United States*

Complete contact information is available at:
https://pubs.acs.org/10.1021/acs.chemrestox.2c00157

Author Contributions

Design and preparation of materials: N.F. and V.S.; *in vitro* data generation and data analyses: M.B., H.M., and V.S.; zebrafish studies: A.N.; mouse inhalation studies, G.B. and A.C.; rabbit cyanide injection studies: J.L., S.M., and M.B.; mouse muscle toxicity and PK analysis: G.K., V.S., and M.B.; cardiotoxicity: K.S.; and manuscript preparation, review, and edits: M.B., V.J.D., R.P., C.M., and G.K.

Notes

The authors declare the following competing financial interest(s): V. J. Davisson is cofounder and CSO of Amplified Sciences, INC.

ABBREVIATIONS

DMSO	dimethylsulfoxide
HCP	sodium hexachloroplatinate
PBS	phosphate-buffered saline
IP	intraperitoneal
ESI-MS	electrospray ionization mass spectrometry
NMR	nuclear magnetic resonance
TLC	thin-layer chromatography
HPLC	high-performance liquid chromatography
UV−Vis	ultraviolet−visible spectroscopy
ISE	ion-selective electrode
XRF	X-ray fluorescence
AUC	area under the curve
FBS	fetal bovine serum
HEPES	4-(2-hydroxyethyl)-1-piperazine ethanesulfonic acid

REFERENCES

(1) Hendry-Hofer, T. B.; Ng, P. C.; Witeof, A. E.; Mahon, S. B.; Brenner, M.; Boss, G. R.; Bebarta, V. S. A Review on Ingested Cyanide: Risks, Clinical Presentation, Diagnostics, and Treatment Challenges. *J. Med. Toxicol.* **2019**, *15*, 128−133.

(2) Gracia, R.; Shepherd, G. Cyanide Poisoning and Its Treatment. *Pharmacotherapy* **2004**, *24*, 1358−1365.

(3) Alarie, Y. Toxicity of Fire Smoke. *Crit. Rev. Toxicol.* **2002**, *32*, 259−289.

(4) Bhattacharya, R.; Flora, S. J. S.Cyanide Toxicity and Its Treatment. In *In Handbook of Toxicology of Chemical Warfare Agents*; Elsevier, 2015; pp 301−314.

(5) Lawson-Smith, P.; Jansen, E. C.; Hyldegaard, O. Cyanide Intoxication as Part of Smoke Inhalation - a Review on Diagnosis and Treatment from the Emergency Perspective. *Scand. J. Trauma Resuscitation Emerg. Med.* **2011**, *19*, No. 14.

(6) Hall, A. H.; Borron, S. W.Smoke Inhalation. In *Toxicology of Cyanides and Cyanogens*; Hall, A. H.; Isom, G. E.; Rockwood, G. A., Eds.; John Wiley & Sons, Ltd, 2015; pp 151−157.

(7) Dal Ponte, S. T.; Dornelles, C. F. D.; Arquilla, B.; Bloem, C.; Roblin, P. Mass-Casualty Response to the Kiss Nightclub in Santa Maria, Brazil. *Prehospital Disaster Med.* **2015**, *30*, 93−96.

(8) Guidotti, T. L.Occupational Exposure to Cyanide. In *Toxicology of Cyanides and Cyanogens*; Hall, A. H.; Isom, G. E.; Rockwood, G. A., Eds.; John Wiley & Sons, Ltd, 2015; pp 158−165.

(9) Ganesan, K.; Raza, S. K.; Vijayaraghavan, R. Chemical Warfare Agents. *J. Pharm. Bioallied Sci.* **2010**, *2*, 166−178.

(10) Pita, R.Cyanide in Chemical Warfare and Terrorism. In *Toxicology of Cyanides and Cyanogens*; Hall, A. H.; Isom, G. E.; Rockwood, G. A., Eds.; John Wiley & Sons, Ltd, 2015; pp 195−208.

(11) Fleischman, R. J.; Lundquist, M.; Jui, J.; Newgard, C. D.; Warden, C. Predicting Ambulance Time of Arrival to the Emergency Department Using Global Positioning System and Google Maps. *Prehospital Emerg. Care* **2013**, *17*, 458−465.

(12) Hall, A. H.Brief Overview of Mechanisms of Cyanide Antagonism and Cyanide Antidotes in Current Clinical Use. In *Toxicology of Cyanides and Cyanogens*; MD, A. H. H. B.; BPharm, G. E. I.; MS, G. A. R. B., Eds.; John Wiley & Sons, Ltd, 2015; pp 283−287.

(13) Marrs, T. C.; Thompson, J. P. The Efficacy and Adverse Effects of Dicobalt Edetate in Cyanide Poisoning. *Clin. Toxicol.* **2016**, *54*, 609−614.

(14) Hall, A. H.Cyanide Antidotes in Clinical Use: Dicobalt EDTA (Kelocyanor). In *Toxicology of Cyanides and Cyanogens*; Hall, A. H.; Isom, G. E.; Rockwood, G. A., Eds.; John Wiley & Sons, Ltd, 2015; pp 292−295.

(15) Shepherd, G.; Velez, L. I. Role of Hydroxocobalamin in Acute Cyanide Poisoning. *Ann. Pharmacother.* **2008**, *42*, 661−669.

(16) Cronican, A. A.; Frawley, K. L.; Straw, E. P.; Lopez-Manzano, E.; Praekunatham, H.; Peterson, J.; Pearce, L. L. A Comparison of the Cyanide-Scavenging Capabilities of Some Cobalt-Containing Complexes in Mice. *Chem. Res. Toxicol.* **2018**, *31*, 259−268.

(17) Brenner, M.; Kim, J. G.; Mahon, S. B.; Lee, J.; Kreuter, K. A.; Blackledge, W.; Mukai, D.; Patterson, S.; Mohammad, O.; Sharma, V. S.; Boss, G. R. Intramuscular Cobinamide Sulfite in a Rabbit Model of Sub-Lethal Cyanide Toxicity. *Ann. Emerg. Med.* **2010**, *55*, 352−363.

(18) Bebarta, V. S.; Tanen, D. A.; Boudreau, S.; Castaneda, M.; Zarzabal, L. A.; Vargas, T.; Boss, G. R. Intravenous Cobinamide versus Hydroxocobalamin for Acute Treatment of Severe Cyanide

Poisoning in a Swine (Sus Scrofa) Model. *Ann. Emerg. Med.* **2014**, *64*, 612−619.

(19) Chan, A.; Balasubramanian, M.; Blackledge, W.; Mohammad, O. M.; Alvarez, L.; Boss, G. R.; Bigby, T. D. Cobinamide Is Superior to Other Treatments in a Mouse Model of Cyanide Poisoning. *Clin. Toxicol.* **2010**, *48*, 709−717.

(20) Lee, J.; Mahon, S. B.; Mukai, D.; Burney, T.; Katebian, B. S.; Chan, A.; Bebarta, V. S.; Yoon, D.; Boss, G. R.; Brenner, M. The Vitamin B12 Analog Cobinamide Is an Effective Antidote for Oral Cyanide Poisoning. *J. Med. Toxicol.* **2016**, *12*, 370−379.

(21) Petrikovics, I.; Budai, M.; Kovacs, K.; Thompson, D. E. Past, Present and Future of Cyanide Antagonism Research: From the Early Remedies to the Current Therapies. *World J. Methodol.* **2015**, *5*, 88−100.

(22) Patterson, S. E.; Moeller, B.; Nagasawa, H. T.; Vince, R.; Crankshaw, D. L.; Briggs, J.; Stutelberg, M. W.; Vinnakota, C. V.; Logue, B. A. Development of Sulfanegen for Mass Cyanide Casualties. *Ann. N. Y. Acad. Sci.* **2016**, *1374*, 202−209.

(23) Kovacs, K.; Duke, A. C.; Shifflet, M.; Winner, B.; Lee, S. A.; Rockwood, G. A.; Petrikovics, I. Parenteral Dosage Form Development and Testing of Dimethyl Trisulfide, as an Antidote Candidate to Combat Cyanide Intoxication. *Pharm. Dev. Technol.* **2017**, *22*, 958−963.

(24) Chan, A.; Lee, J.; Bhadra, S.; Bortey-Sam, N.; Hendry-Hofer, T. B.; Bebarta, V. S.; Mahon, S. B.; Brenner, M.; Logue, B.; Pilz, R. B.; Boss, G. R. Development of Sodium Tetrathionate as a Cyanide and Methanethiol Antidote. *Clin. Toxicol.* **2022**, *60*, 332−341.

(25) Thompson, A.; Dunn, M.; Jefferson, R. D.; Dissanayake, K.; Reed, F.; Gregson, R.; Greenhalgh, S.; Clutton, R. E.; Blain, P. G.; Thomas, S. H.; Eddleston, M. Modest and Variable Efficacy of Pre-Exposure Hydroxocobalamin and Dicobalt Edetate in a Porcine Model of Acute Cyanide Salt Poisoning. *Clin. Toxicol.* **2020**, *58*, 190−200.

(26) Hall, A. H.; Rumack, B. H. Clinical Toxicology of Cyanide. *Ann. Emerg. Med.* **1986**, *15*, 1067−1074.

(27) *Toxicology of Cyanides and Cyanogens*, 1st ed.; John Wiley & Sons, Ltd, 2015; pp 333−347.

(28) Thompson, J. P.; Marrs, T. C. Hydroxocobalamin in Cyanide Poisoning. *Clin. Toxicol.* **2012**, *50*, 875−885.

(29) Nath, A. K.; Shi, X.; Harrison, D. L.; Morningstar, J. E.; Mahon, S.; Chan, A.; Sips, P.; Lee, J.; MacRae, C. A.; Boss, G. R.; Brenner, M.; Gerszten, R. E.; Peterson, R. T. Cisplatin Analogs Confer Protection against Cyanide Poisoning. *Cell Chem. Biol.* **2017**, *24*, 565−575.e4.

(30) Wasylishen, R. E.; Britten, J. F. Relaxation of Platinum−195 in Tetracyanoplatinate(II) and Hexacyanoplatinate(IV) in Aqueous Solutions. *Magn. Reson. Chem.* **1988**, *26*, 1075−1078.

(31) Wang, X.-B.; Wang, Y.-L.; Woo, H.-K.; Li, J.; Wu, G.-S.; Wang, L.-S. Free Tetra- and Hexa-Coordinated Platinum-Cyanide Dianions, Pt(CN)42- and Pt(CN)62-: A Combined Photodetachment Photoelectron Spectroscopic and Theoretical Study. *Chem. Phys.* **2006**, *329*, 230−238.

(32) Smith, R. M.; Martell, A. E.*Critical Stability Constants*; Springer Book Archive, 1976.

(33) Varbanov, H. P.; Ortiz, D.; Höfer, D.; Menin, L.; Galanski, M.; Keppler, B. K.; Dyson, P. J. Oxaliplatin Reacts with DMSO Only in the Presence of Water. *Dalton Trans.* **2017**, *46*, 8929−8932.

(34) Hall, M. D.; Telma, K. A.; Chang, K.-E.; Lee, T. D.; Madigan, J. P.; Lloyd, J. R.; Goldlust, I. S.; Hoeschele, J. D.; Gottesman, M. M. Say No to DMSO: Dimethylsulfoxide Inactivates Cisplatin, Carboplatin, and Other Platinum Complexes. *Cancer Res.* **2014**, *74*, 3913−3922.

(35) Summa, N.; Schiessl, W.; Puchta, R.; van Eikema Hommes, N.; van Eldik, R. Thermodynamic and Kinetic Studies on Reactions of Pt(II) Complexes with Biologically Relevant Nucleophiles. *Inorg. Chem.* **2006**, *45*, 2948−2959.

(36) Farrell, N. Dimethyl Sulphoxide as Leaving Group: Applications in Transition Metal Chemotherapy. *J. Chem. Soc., Chem. Commun.* **1982**, No. 331.

(37) Morningstar, J.; Lee, J.; Hendry-Hofer, T.; Witeof, A.; Lyle, L. T.; Knipp, G.; MacRae, C. A.; Boss, G. R.; Peterson, R. T.; Davisson, V. J.; Gerszten, R. E.; Bebarta, V. S.; Mahon, S.; Brenner, M.; Nath, A. K. Intramuscular Administration of Hexachloroplatinate Reverses Cyanide-Induced Metabolic Derangements and Counteracts Severe Cyanide Poisoning. *FASEB BioAdv.* **2019**, *1*, 81−92.

(38) Braddock, P. D.; Connors, T. A.; Jones, M.; Khokhar, A. R.; Melzack, D. H.; Tobe, M. L. Structure and Activity Relationships of Platinum Complexes with Anti-Tumour Activity. *Chem.-Biol. Interact.* **1975**, *11*, 145−161.

(39) Hall, M. D.; Telma, K. A.; Chang, K.-E.; Lee, T. D.; Madigan, J. P.; Lloyd, J. R.; Goldlust, I. S.; Hoeschele, J. D.; Gottesman, M. M. Say No to DMSO: Dimethylsulfoxide Inactivates Cisplatin, Carboplatin, and Other Platinum Complexes. *Cancer Res.* **2014**, *74*, 3913−3922.

(40) Fischer, S. J.; Benson, L. M.; Fauq, A.; Naylor, S.; Windebank, A. J. Cisplatin and Dimethyl Sulfoxide React to Form an Adducted Compound with Reduced Cytotoxicity and Neurotoxicity. *Neurotoxicology* **2008**, *29*, 444−452.

(41) Sundquist, W. I.; Ahmed, K. J.; Hollis, L. S.; Lippard, S. J. Solvolysis Reactions of Cis- and Trans-Diamminedichloroplatinum-(II) in Dimethyl Sulfoxide. Structural Characterization and DNA Binding of Trans-Bis(Ammine)Chloro(DMSO)Platinum(1+). *Inorg. Chem.* **1987**, *26*, 1524−1528.

(42) Kerrison, S. J. S.; Sadler, P. J. Solvolysis of Cis-[Pt(NH3)2Cl2] in Dimethyl Sulphoxide and Reactions of Glycine with [PtCl3-(Me2SO)]− as Probed by 195Pt Nuclear Magnetic Resonance Shifts and 195Pt−15N Coupling Constants. *J. Chem. Soc. Chem. Commun.* **1977**, 861−863.

(43) Jovanović, S.; Petrović, B.; Bugarčić, Ž. D.; van Eldik, R. Reduction of Some Pt(IV) Complexes with Biologically Important Sulfur-Donor Ligands. *Dalton Trans.* **2013**, *42*, 8890−8896.

(44) Norman, R. E.; Ranford, J. D.; Sadler, P. J. Studies of Platinum(II) Methionine Complexes: Metabolites of Cisplatin. *Inorg. Chem.* **1992**, *31*, 877−888.

(45) Li, C.; Li, Z.; Sletten, E.; Arnesano, F.; Losacco, M.; Natile, G.; Liu, Y. Methionine Can Favor DNA Platination by Trans-Coordinated Platinum Antitumor Drugs. *Angew. Chem.* **2009**, *121*, 8649−8652.

(46) Zimmermann, T.; Burda, J. V. Reactions of Cisplatin with Cysteine and Methionine at Constant PH; a Computational Study. *Dalton Trans.* **2010**, *39*, 1295−1301.

(47) Zimmermann, T.; Chval, Z.; Burda, J. V. Cisplatin Interaction with Cysteine and Methionine in Aqueous Solution: Computational DFT/PCM Study. *J. Phys. Chem. B* **2009**, *113*, 3139−3150.

(48) Li, C.; Huang, R.; Ding, Y.; Sletten, E.; Arnesano, F.; Losacco, M.; Natile, G.; Liu, Y. Effect of Thioethers on DNA Platination by Trans-Platinum Complexes. *Inorg. Chem.* **2011**, *50*, 8168−8176.

(49) Murdoch, S. d. P.; del, P.; Ranford, J. D.; Sadler, P. J.; Berners-Price, S. J. Cis-Trans Isomerization of [Bis(L-Methioninato)-Platinum]: Metabolite of the Anticancer Drug Cisplatin. *Inorg. Chem.* **1993**, *32*, 2249−2255.

(50) Lopez-Manzano, E.; Cronican, A. A.; Frawley, K. L.; Peterson, J.; Pearce, L. L. Cyanide Scavenging by a Cobalt Schiff-Base Macrocycle: A Cost-Effective Alternative to Corrinoids. *Chem. Res. Toxicol.* **2016**, *29*, 1011−1019.

(51) Bojesen, G.; Hvelplund, P.; Jo/rgensen, T. J. D.; Nielsen, S. B. Probing the Lowest Coordination Number of Dianionic Platinum−Cyanide Complexes in the Gas Phase: Dynamics of the Charge Dissociation Process. *J. Chem. Phys.* **2000**, *113*, 6608−6612.

(52) Mason, W. R.; Gray, H. B. Electronic Structures of Square-Planar Complexes. *J. Am. Chem. Soc.* **1968**, *90*, 5721−5729.

(53) Tolbatov, I.; Marzo, T.; Cirri, D.; Gabbiani, C.; Coletti, C.; Marrone, A.; Paciotti, R.; Messori, L.; Re, N. Reactions of Cisplatin and Cis-[PtI2(NH3)2] with Molecular Models of Relevant Protein Sidechains: A Comparative Analysis. *J. Inorg. Biochem.* **2020**, *209*, No. 111096.

(54) Li, H.; Snelling, J. R.; Barrow, M. P.; Scrivens, J. H.; Sadler, P. J.; O'Connor, P. B. Mass Spectrometric Strategies to Improve the

Identification of Pt(II)-Modification Sites on Peptides and Proteins. *J. Am. Soc. Mass Spectrom.* **2014**, *25*, 1217−1227.

(55) Pinato, O.; Musetti, C.; Sissi, C. Pt-Based Drugs: The Spotlight Will Be on Proteins. *Metallomics* **2014**, *6*, 380−395.

(56) Casini, A.; Reedijk, J. Interactions of Anticancer Pt Compounds with Proteins: An Overlooked Topic in Medicinal Inorganic Chemistry? *Chem. Sci.* **2012**, *3*, 3135−3144.

(57) Burns, C. G.; Milan, D. J.; Grande, E. J.; Rottbauer, W.; MacRae, C. A.; Fishman, M. C. High-Throughput Assay for Small Molecules That Modulate Zebrafish Embryonic Heart Rate. *Nat. Chem. Biol.* **2005**, *1*, 263−264.

(58) Milan, D. J.; Peterson, T. A.; Ruskin, J. N.; Peterson, R. T.; MacRae, C. A. Drugs That Induce Repolarization Abnormalities Cause Bradycardia in Zebrafish. *Circulation* **2003**, *107*, 1355−1358.

(59) Brenner, M.; Mahon-Brenner, S.; Patterson, S. E.; Rockwood, G. A.; Boss, G. R.Cyanide Antidotes in Development and New Methods to Monitor Cyanide Toxicity. In *Toxicology of Cyanides and Cyanogens*; MD, A. H. H. B.; BPharm, G. E. I.; MS, G. A. R. B., Eds.; John Wiley & Sons, Ltd, 2015; pp 309−316.

(60) Richens, D. T. Ligand Substitution Reactions at Inorganic Centers. *Chem. Rev.* **2005**, *105*, 1961−2002.

(61) Blumenthal, D. C.; Kassner, R. J. Cyanide Binding to the Cytochrome c Ferric Heme Octapeptide. A Model for Anion Binding to the Active Site of High Spin Ferric Heme Proteins. *J. Biol. Chem.* **1980**, *255*, 5859−5863.

(62) Cronican, A. A.; Frawley, K. L.; Straw, E. P.; Lopez-Manzano, E.; Praekunatham, H.; Peterson, J.; Pearce, L. L. A Comparison of the Cyanide-Scavenging Capabilities of Some Cobalt-Containing Complexes in Mice. *Chem. Res. Toxicol.* **2018**, *31*, 259−268.

(63) Chan, A.; Jiang, J.; Fridman, A.; Guo, L. T.; Shelton, G. D.; Liu, M.-T.; Green, C.; Haushalter, K. J.; Patel, H. H.; Lee, J.; Yoon, D.; Burney, T.; Mukai, D.; Mahon, S. B.; Brenner, M.; Pilz, R. B.; Boss, G. R. Nitrocobinamide, a New Cyanide Antidote That Can Be Administered by Intramuscular Injection. *J. Med. Chem.* **2015**, *58*, 1750−1759.